The Role of Loop F Residues in Determining Differential *d*-Tubocurarine Potencies in Mouse and Human 5-Hydroxytryptamine 3A Receptors†

Ran Zhang,[‡,§,▽] Xiaofei Wen,[‡,▽] Julius Militante,[‡,⊥] Brent Hester,[‡,#] Heather E. Rhubottom,[§] Hongwei Sun,[‡,Δ] Nancy J. Leidenheimer,[+] Dong Yan,[||] Michael M. White,[||] and Tina K. Machu*[,‡,§]

Department of Pharmacology and Neuroscience, Texas Tech University Health Sciences Center, 3601 Fourth Street, Lubbock, Texas 79430, Texas Department of Public Safety, 1302 Mac Davis Lane, Lubbock, Texas 79401, Department of Pharmacology and Neuroscience, University of North Texas Health Science Center, 3500 Camp Bowie Boulevard, Fort Worth, Texas 76107-2699, Department of Experimental Therapeutics, The University of Texas M.D. Anderson Cancer Center, 1515 Holcombe Boulevard, Houston, Texas 77030-4009, Department of Biochemistry, Louisiana State University Medical Center, 1501 Kings Highway, Shreveport, Louisiana 71130-3932, Department of Biochemistry and Molecular Biology, Drexel University College of Medicine, 245 North 15th Street, Philadelphia, Pennsylvania 19102, Department of Anesthesiology, Washington University School of Medicine, 660 South Euclid Drive, St. Louis, Missouri 63110

Received August 8, 2006; Revised Manuscript Received November 3, 2006

ABSTRACT: The competitive antagonist *d*-tubocurarine (curare) has greater potency at mouse than at human 5-hydroxytryptamine 3A (5-HT_{3A}) receptors, despite 84% amino acid sequence identity between the receptors. Within the ligand binding domain of this receptor are six loops (A−F). A previous report demonstrated that loop C of the 5-HT_{3A} receptor contributed to differential potency between the receptors [Hope, A. G. et al. (1999) *Mol. Pharmacol. 55*, 1037−1043]. The present study tested the hypothesis that loop F plays a significant role in conferring interspecies curare potency differences. Wild-type, chimeric, and point mutant 5-HT_{3A} receptors were expressed in *Xenopus* oocytes, and two-electrode voltage clamp electrophysiological recordings were performed. Our data suggest that loops C and F contribute to curare potency, given that the curare IC_{50}'s (concentration of drug that produces 50% inhibition of the response) for chimeric human receptors with substitutions of mouse residues in loop C (40.07 ± 2.52 nM) or loop F (131.8 ± 5.95 nM) were intermediate between those for the mouse (12.99 ± 0.77 nM) and human (1817 ± 92.36 nM) wild-type receptors. Two human point mutant receptors containing mouse receptor substitutions in loop F (H-K195E or H-V202I) had significantly lower curare IC_{50}'s than that of the human receptor. The human double mutant receptor, H-K195E,V202I, had the same curare IC_{50} (133.8 ± 6.38 nM) as that of the human receptor containing all six loop F mouse substitutions. These results demonstrate that two loop F residues make a significant contribution in determining curare potency at the 5-HT_{3A} receptor.

The 5-HT_3[1] receptor is a member of the Cys-loop superfamily of ligand-gated ion channels (LGICs) and mediates excitatory fast synaptic transmission in the central and peripheral nervous systems (*1*). Of the five subunits (A−E) cloned to date, only 5-HT_{3A} and 5-HT_{3B} subunits have been demonstrated to have functional significance in the central or peripheral nervous systems (*1*−*5*). The 5-HT_{3B} subunit must be coexpressed with the 5-HT_{3A} subunit to be functional (*2*, *3*), but sole expression of the 5-HT_{3A} subunit yields functional homomeric receptors. The A homomer is the predominant form of the 5-HT_3 receptor in rodent brain (*6*).

All members of the Cys-loop family of LGICs are pentameric in structure and contain at least two agonist binding domains that are situated at the interface of two subunits in the extracellular N-termini (reviewed in ref *7*). One subunit contains the principal component of the ligand binding domain, loops A, B, and C. The other subunit contains the complementary component, loops D, E, and F. Binding of ligand causes a series of conformational changes that result in ion channel opening. Previous studies in *Torpedo californica* and mouse nicotinic acetylcholine (nACh) receptors, which have laid much of the groundwork

† This work was supported by NS 43438 to T.K.M. and a Grant-in-Aid from the American Heart Association Pennsylvania-Delaware Affiliate to M.M.W.

* To whom correspondence should be addressed. Mailing address: Department of Pharmacology and Neuroscience, University of North Texas Health Science Center, 3500 Camp Bowie Blvd., Fort Worth, Texas 76107-2699. Phone: 817-735-2356. Fax: 817-735-0408. E-mail: tmachu@hsc.unt.edu.

‡ Texas Tech University Health Sciences Center.

§ University of North Texas Health Science Center.

▽ Contributed equally to the work.

⊥ Washington University School of Medicine.

Texas Department of Public Safety.

Δ The University of Texas M.D. Anderson Cancer Center.

+ Louisiana State University Medical Center.

|| Drexel University College of Medicine.

[1] Abbreviations: curare, *d*-tubocurarine; 5-HT, 5-hydroxytryptamine (serotonin); 5-HT_{3A}, 5-hydroxytryptamine 3A receptor; LGIC, ligand-gated ion channel; nACH, nicotinic acetylcholine; DMC, dimethyl-*d*-tubocurarine; AChBP, acetylcholine binding protein; MBS, modified Barth's solution; HEPES, *N*-2-hydroxyethylpiperazine-*N*′-2-ethanesulfonic acid; EC_{50}, concentration of drug that produces a 50% response; EC_{10}, concentration of drug that produces a 10% response; IC_{50}, concentration of drug that produces 50% inhibition of the response.

10.1021/bi0616100 CCC: $37.00
Published on Web 01/13/2007

for studies of ligand recognition in the 5-HT$_{3A}$ receptor, identified residues in the α, *γ*, and *δ* subunits that are crucial for agonist or antagonist binding through a variety of biochemical and electrophysiological approaches (reviewed in ref *8*). With respect to curare, several residues in the principal α subunit have been identified (*9*−*12*); in the complementary component, amino acids in both loops E and F are responsible for the high (*γ* subunit) versus low (*δ* subunit) curare or dimethyl-*d*-tubocurarine (DMC) affinity mediated by the two nonequivalent interfaces in the receptor (*13*, *14*). A study employing mutant thermodynamic cycle analysis with curare analogs has demonstrated that the quaternary 2′ N likely interacts with Tyr117 in the *γ* subunit (*15*).

Numerous investigations of ligand recognition in the 5-HT$_{3A}$ receptor have utilized a strategy of examining receptors with amino acids mutagenized to alanine or other residues that differ in selected physicochemical properties. In ligand binding and electrophysiological studies, a number of residues that are involved in mediating agonist or antagonist or both affinity or potency have been determined. A number of studies have focused on loop C and its role in ligand binding, as well as its likely contribution to gating (*16*−*19*). In loops A, B, D, and E, mutation of aromatic, as well as charged, amino acids also revealed critical residues for ligand binding, gating, and surface expression (*17*, *20*−*28*). In contrast, less work has been done on loop F of the 5-HT$_{3A}$ receptor. Thompson et al. (*19*) reported that three mutations in loop F (W195A, S203A, and S206A) alter [^{3}H]-granisetron binding. Thompson et al. (*29*) investigated 21 mutations inclusive of and near loop F and found that two regions displayed increases in K_d values for ^{3}H-granisetron. Common to these studies is the observation that mutations do not affect ligand recognition uniformly, suggesting that ligands have different points of contact with the agonist binding domain. A very significant advance in the field occurred with the crystallization of the acetylcholine binding protein (AChBP), a structural homolog of the N-terminal domains of the LGIC superfamily (*30*). Homology modeling of the 5-HT$_{3A}$ receptor ligand binding domain, with information obtained from mutagenesis studies used as a guide, has allowed investigators to dock specific ligands in and approximate the three-dimensional architecture of the binding pocket (*18*, *27*, *28*, *31*, *32*).

In the present study, we have used interspecies chimeras and point mutant receptors to identify residues involved in determining curare potency in mouse and human 5-HT$_{3A}$ receptors. It has long been known that 5-HT$_3$ receptors from different mammalian species display differential sensitivities to drugs such as curare, 2-methyl 5-HT, and *m*-chlorophenylbiguanide (reviewed in ref *33*). However, cloning of 5-HT$_{3A}$ receptors from six species revealed a high degree of amino acid conservation among the receptors (*1*, *34*−*38*). Several investigators have examined interspecies chimeras and, in some cases, point mutant receptors containing corresponding amino acids (*37*−*40*). In all studies, loop C domains were identified as contributing to interspecies differences in drug action. In particular, Hope et al. (*39*) demonstrated that loop C contributed to part but not all of the large difference in potency of the competitive antagonist curare at mouse and human 5-HT$_{3A}$ receptors. In electrophysiological recordings conducted in wild-type, chimeric,

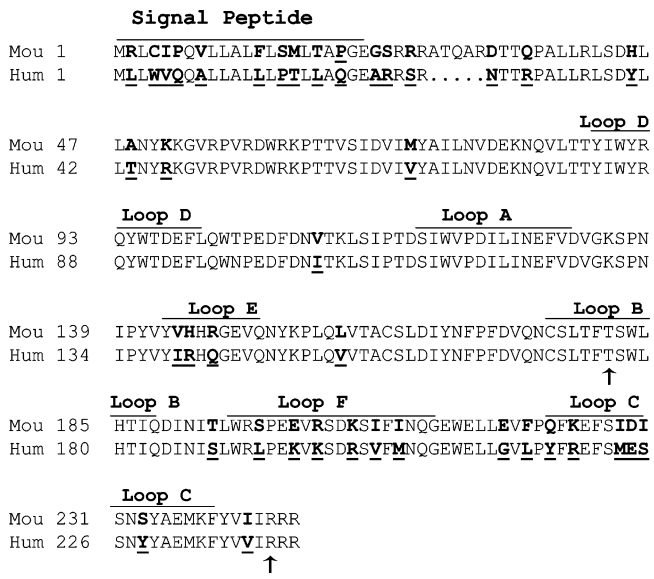

FIGURE 1: The N-terminal domains of the mouse and human 5-HT$_{3A}$ receptors are aligned, and numbering begins with the initiating methionine. The signal peptide is indicated. Loops A−F correspond to loops in the muscle nACh receptor, which have been identified as contributing to the ligand binding domain (reviewed in ref *8*). Loops A−C are localized in the principal component, and loops D−F are present in the complementary component. The black arrows indicate the switch points for the chimeras in which the distal one-third of the N-terminus has been substituted in the mouse and human receptors (M181H239M and H176M244H). Smaller chimeras within the distal one-third of the N-temini were generated. Loop C+1 chimeras contain loop C receptor substitutions and the isoleucine to valine or valine to isoleucine substitution that is C-terminal to loop C and immediately N-terminal to TM1. Loop F chimeras contain the six loop F substitutions, whereas the loop F+3 chimeras contain the loop F substitutions and the three substitutions that are N-terminal or C-terminal to loop F.

and corresponding point mutant 5-HT$_{3A}$ receptors expressed in *Xenopus* oocytes, we have determined that loop C and loop F of mouse and human 5-HT$_{3A}$ receptors fully account for the approximately 140-fold greater potency of curare at the mouse receptor. Furthermore, two residues, Lys195 and Val202 in the human receptor, and the orthologs, Glu200 and Ile207 in the mouse receptor, underlie the role of loop F in conferring curare potency. Thus, the work presented in the current study identifies the role of two previously uncharacterized loop F amino acids that change curare potency and thus may play a role in ligand recognition in the 5-HT$_{3A}$ receptor.

EXPERIMENTAL PROCEDURES

Construction of Chimeric and Point Mutant Receptor cDNAs and cRNAs. Mouse and human 5-HT$_{3A}$ receptor cDNAs, provided by Drs. D. Julius and A. Miyake, respectively, were subcloned into pBluescript KS$^-$ and pCR-Script Amp SK(+)$^-$ (Stratagene, La Jolla, CA). Numbering of the amino acids in the two receptors began with the initiating methionine. Two unique restriction enzyme cleavage sites, *Spe*I, and *Nar*I, were introduced in both mouse and human 5-HT$_{3A}$ receptor cDNAs by site-directed mutagenesis (U.S.E. mutagenesis kit, Pharmacia Biotech Inc., Piscataway, NJ) of the nucleotides encoding the conserved residues Thr181 and Arg244 in the mouse receptor cDNA and Thr176 and Arg239 in the human receptor cDNA (Figure 1). Chimeric receptors were named by species, junction point,

species, junction point, and species. For example, H176M244H contains human receptor residues 1−176, mouse receptor residues through 244, and the balance human receptor residues. Both receptor cDNAs were digested with the restriction enzymes, and the appropriate fragments were ligated to generate chimeric receptors in which the distal one-third of the N-termini containing loops C and F were swapped. Point mutations were introduced in mouse and human receptor cDNAs with the U.S.E. mutagenesis kit. Chimeras containing loop F, loop F+3, or loop C+1 substitutions were generated with multiple rounds of mutagenesis, in which one to three substitutions were made simultaneously. Chimeric and point mutant receptor cDNAs were confirmed by dideoxynucleotide sequencing at the Biotechnology Core Facility at Texas Tech University, Lubbock, TX. The cDNAs were transcribed with the T3 mMESSAGE mMACHINE (Ambion, Austin, TX), and oocytes were microinjected with cRNAs.

Receptor Expression and Electrophysiological Recordings. Oocytes obtained from *Xenopus laevis* frogs were subjected to chemical separation and defolliculation as previously described (*41*). Oocytes were incubated at room temperature in ND96 media, containing (in mM) NaCl 96, KCl 2, $CaCl_2$ 1.8, $MgCl_2$ 1, and HEPES 5 (pH 7.5), plus 10 mg/L streptomycin, 50 mg/L gentamicin, 10 000 units/L penicillin, 96 mg/L sulfamethoxazole, 19 mg/L trimethoprim, 0.5 mM theophylline, and 2 mM sodium pyruvate.

5-HT-elicited currents were recorded in the two-electrode voltage clamp configuration in oocytes on days 2 through 7 following injection (*41*). Serotonin and curare were obtained from Sigma (St. Louis, MO) and were dissolved in modified Barth's solution (MBS) containing (in mM) NaCl 88, KCl 1, $NaHCO_3$ 2.4, HEPES 10, $MgSO_4$ 0.82, $Ca(NO_3)_2$ 0.33, and $CaCl_2$ 0.91 (pH 7.5). Serotonin was applied in the absence or presence of curare at 2 mL/min for 30 s to 1 min.

Data Analysis. In all experiments, peak current amplitudes were measured. The control values were obtained by averaging the 5-HT-mediated responses obtained before and after the response to 5-HT plus curare. For generation of 5-HT concentration response curves, currents were expressed as a percentage of the maximal 5-HT (25 μM) responses. For antagonism by curare, percent inhibition was calculated by subtracting the current obtained from 5-HT plus curare from the average current obtained with 5-HT alone; the difference was divided by the average 5-HT-mediated current, and the quotient was multiplied by 100.

Graphpad Prism (San Diego, CA) was used to calculate EC_{50}'s, IC_{50}'s, and Hill coefficients. The equation used to calculate these parameters was: $I/I_{control} = 1/[1 + [D/EC_{50}]^n]$, where I is current, $I_{control}$ is the control current, D is the drug concentration, EC_{50} is the concentration of drug that produces 50% of the maximal response, IC_{50} is the concentration of drug that produces 50% inhibition of the response, and n is the Hill coefficient. One-way analysis of variance (ANOVA) and Student−Newman−Keul's post-hoc analyses were performed by Instat (San Diego, CA).

In the double mutant thermodynamic cycle analysis, change in Gibbs free energy (ΔG) was calculated: $\Delta G = -RT \ln(IC_{50}^{single-mutant}/IC_{50}^{wild-type})$ or $\Delta G = -RT \ln(IC_{50}^{double-mutant}/IC_{50}^{single-mutant})$, where R is the gas constant and T is the room temperature in kelvin (reviewed in ref *42*). It should be noted that the IC_{50} value determined in functional experiments is not a pure measure of antagonist affinity (*43*), so changes in IC_{50} may not have a 1:1 correspondence to changes in affinity.

Molecular Modeling and Ligand Docking. A structural model of the extracellular domain of the mouse $5HT_{3A}$ receptor was generated using version 8.2 of the program MODELLER (*44*), using the X-ray structure of the apo protein (Protein Data Bank ID 2BYN) and the antagonist methyllycaconitine-bound form of the *Aplysia* AChBP (Protein Data Bank ID 2BYR) (*45*) as templates as described previously (*27*, *28*). The loop F region, which has insertions relative to the template sequence, was further refined using MODELLER, and then side chains were refined using SCWRL 3.0 (*46*). Models were evaluated using ProSa2003 (*47*), and the highest scoring models were used for docking simulations.

Curare was docked to each binding site in the model using Autodock 3.05 (*48*). Solvation parameters were added to the protein coordinate file and the ligand torsions were defined using the "Addsol" and "Autotors" utilities, respectively, in Autodock 3.05. Gasteiger−Marsili charges, which use the united atom representation for nonpolar hydrogens, were applied to ligands prior to docking (*49*). The docking was performed with the initial population size set to 100 with 100 independent runs using otherwise default parameters in the standard protocol on a 30 Å × 30 Å × 40 Å grid with spacing of 0.375 Å. The size of the grid gives sufficient freedom for the ligands to be docked in all possible orientations while not permitting them to move outside of the binding site. In addition to returning the docked structure, AutoDock also calculates an affinity constant for each ligand−receptor configuration. AutoDock allows flexibility in the ligand. While the scoring functions used in AutoDock can discriminate between near-native and misdocked conformations of a ligand (*50*), AutoDock can return several different conformations of the ligand in the binding site. However, the models that we used in this study were the ones validated in our laboratory using double-mutant cycle analysis (*28*) and thus likely represent the actual situation. Images were produced using the UCSF Chimera package (*51*) from the Computer Graphics Laboratory, University of California, San Francisco (supported by NIH P41 RR-01081).

RESULTS

A previous study demonstrated that loop C of the ligand binding domain of the $5\text{-}HT_{3A}$ receptor accounted for part but not all of the large difference in potency of the competitive antagonist curare at mouse and human $5\text{-}HT_{3A}$ receptors (*39*). An alignment of the N-terminal domains of mouse and human $5\text{-}HT_{3A}$ receptors (Figure 1) revealed that the distal one-third of the N-termini, in which loops C and F are present, contains the majority of differences in amino acid composition. Among the other loops of the ligand binding domain, only loop E contains differences in amino acid sequence between mouse and human receptors. Therefore, the present study evaluated amino acids in the distal one-third of the N-termini for their roles in determining curare potency in mouse and human $5\text{-}HT_{3A}$ receptors. A series of interspecies chimeras, in which the distal one-third

Table 1: 5-HT and Curare Potencies at Wild-Type, Chimeric, and Point Mutant Mouse and Human 5-HT_{3A} Receptors

receptor	5-HT EC_{50} (mean ± SE) μM	5-HT Hill slope (mean ± SE)	curare IC_{50} (mean ± SE) nM	curare Hill slope (mean ± SE)
mouse WT	1.02 ± 0.07	2.23 ± 0.37	12.99 ± 0.77	1.17 ± 0.09
M181H239M	1.20 ± 0.03	2.86 ± 0.14	1689 ± 115.24	1.33 ± 0.13
M-loop C+1	3.93 ± 0.22[a]	2.12 ± 0.29	137.6 ± 7.93[a,b]	1.30 ± 0.10
M-loop F	3.66 ± 0.04[a]	2.64 ± 0.10	76.97 ± 3.52[a,b]	1.54 ± 0.10
M-loop F+3	2.92 ± 0.13[a]	2.65 ± 0.42	86.27 ± 5.11[a,b]	1.34 ± 0.13
M-loop C+1,E200K,I207V	2.93 ± 0.23[a]	2.30 ± 0.40	1070 ± 50.8[a,b]	1.42 ± 0.10
human WT	1.46 ± 0.04	3.42 ± 0.31	1817 ± 92.36[e]	1.19 ± 0.08
H176M244H	1.70 ± 0.30	1.97 ± 0.25	8.26 ± 0.62[f]	0.98 ± 0.09
H-loop C+1	3.28 ± 0.12[b]	2.32 ± 0.21	40.07 ± 2.52[a,b]	1.15 ± 0.09
H-loop F	2.36 ± 0.12[c]	2.05 ± 0.17	131.8 ± 5.95[a,b]	1.50 ± 0.10
H-loop F+3	3.04 ± 0.17[b]	2.38 ± 0.31	82.45 ± 3.63[a,b,d]	1.39 ± 0.08
H-K195E,V202I	1.76 ± 0.06	2.17 ± 0.17	133.8 ± 6.38[b]	1.23 ± 0.09
H-loop C+1,V202I	2.20 ± 0.10	2.13 ± 0.21	8.12 ± 0.21	0.99 ± 0.02
H-loop C+1,K195E,V202I	2.40 ± 0.15[c]	1.95 ± 0.29	5.73 ± 0.38	1.09 ± 0.07
H-S188T	2.81 ± 0.16[b]	1.59 ± 0.17	2013 ± 189.00	0.99 ± 0.09
H-L192S	1.95 ± 0.14	1.91 ± 0.30	1615 ± 76.53	1.15 ± 0.07
H-K195E	1.30 ± 0.07	1.30 ± 0.08	546 ± 26.41[b]	1.34 ± 0.10
H-K197R	3.63 ± 0.29[b]	1.76 ± 0.30	1766 ± 41.86	1.37 ± 0.04
H-R200K	4.23 ± 0.33[b]	1.63 ± 0.21	2200 ± 227.48	1.04 ± 0.13
H-V202I	4.27 ± 0.18[b]	2.43 ± 0.25	255.7 ± 7.27[b]	1.35 ± 0.05
H-M204I	2.67 ± 0.18[b]	1.99 ± 0.30	2141 ± 157.92	1.54 ± 0.16
H-G213E	1.48 ± 0.11	1.74 ± 0.23	1676 ± 152.02	1.07 ± 0.11
H-L215F	2.11 ± 0.18	1.65 ± 0.19	1297 ± 40.05[c]	1.27 ± 0.05

[a] $p < 0.001$ compared with mouse WT. [b] $p < 0.001$ compared with human WT. [c] $p < 0.05$ compared with human WT. [d] $p < 0.001$ compared with H-loop F by Student−Newman−Keuls post-hoc analysis; one-way ANOVAs are described in the Results or figure legends. [e] $p < 0.001$ compared with human WT. [f] $p < 0.001$ compared with mouse WT by Student's *t* test.

of the N-termini or smaller domains in the N-termini were exchanged, were examined. A series of point mutant receptors was constructed. As shown in Figure 1, there are six nonconserved residues between mouse and human receptors in loop F. In addition, there is one nonconserved residue between loop B and loop F and two nonconserved residues between loop F and loop C. In the human receptor, each of these nine nonconserved residues was mutated to the corresponding mouse amino acid.

A total of 22 chimeric and point mutant receptors were constructed, including five on the mouse receptor background and 17 on the human receptor background. Along with mouse and human wild-type (WT) receptors, these chimeric and mutant receptors were initially tested for 5-HT potency (Table 1). Among the mouse chimeric receptors EC_{50} values ranged from 1.2 ± 0.03 to 3.93 ± 0.22 μM, compared with the mouse WT EC_{50} of 1.02 ± 0.07 μM. One-way ANOVA of mouse WT and mouse chimeric receptor EC_{50}'s was significant, $p < 0.001$, and all chimeric receptors had significantly greater EC_{50}'s than mouse WT, except M181H239M. Likewise, among the human chimeric and point mutant receptors, there was a significant effect of mutation on 5-HT EC_{50}, one-way ANOVA, $p < 0.001$. Nine of 17 receptors had significantly greater 5-HT EC_{50}'s relative to human WT (1.46 ± 0.04 μM), with the greatest being that of H-V202I, 4.27 ± 0.18 μM, Table 1. It must be pointed out that the largest fold change in 5-HT EC_{50} in the mutant receptors was 3.85 and 2.9 for mouse and human receptors, respectively. Thus, while significant, the changes in EC_{50}'s are modest. These results suggest that the substitutions on either receptor background do not grossly alter the coupling of ligand binding with channel gating.

The contribution of the distal one-third of the N-termini in conferring curare potency was assessed (Figure 2A,B; Table 1). Curare concentration response curves were performed on mouse WT, human WT, M181H239M, and H176M244H receptors, with an EC_{10} concentration of 5-HT. The mouse WT had a curare IC_{50} of 12.99 ± 0.77 nM, and the human WT had a curare IC_{50} of 1817 ± 92 nM, an ~140-fold shift in curare potency. The human receptor chimera, H176M244H, had a curare IC_{50} of 8.26 ± 0.62 nM, which is slightly but significantly less than that of mouse WT (Table 1). Replacement of the distal one-third of N-terminus of the mouse receptor with that of the human receptor (M181H239M) resulted in a receptor with a curare IC_{50} of 1689 ± 115 nM. The curare IC_{50}'s of the two receptors were not significantly different (Table 1). These results suggest that the distal one-third of the N-terminus is sufficient to determine whether the receptor has mouse- or human-like curare potency.

Loops C and F are in the distal one-third of the N-terminus of the 5-HT_{3A} receptor, and each loop was evaluated for its role in determining curare potency. The loop C+1 chimeras contain loop C receptor substitutions plus the single substitution that is C-terminal to loop C and immediately N-terminal to TM1 (H-V237I and M-I244V), Figure 1. Loop F chimeras contain the six loop F substitutions, whereas the loop F+3 chimeras contain the loop F substitutions and the three substitutions that are N-terminal (H-S188T and M-T193S) or C-terminal (H-G213E,L215F and M-E218G,F220L) to loop F, Figure 1. In Figure 3A,B, mouse receptor chimeras containing human receptor orthologs were evaluated. With M-loop C+1, M-loop F, and M-loop F+3, the curare concentration response curves were shifted rightward relative to mouse WT. The IC_{50}'s of M-loop C+1 (137.6 ± 7.93 nM), M-loop F (76.97 ± 3.52 nM), and M-loop F+3 (86.27 ± 5.11 nM) were significantly greater than that of mouse WT, and M-loop F and M-loop F+3 IC_{50}'s were not different from each other (Table 1). Substitution of mouse residues with human receptor orthologs in the mouse chimeric receptors resulted in a 5−10-fold decrease in curare potency,

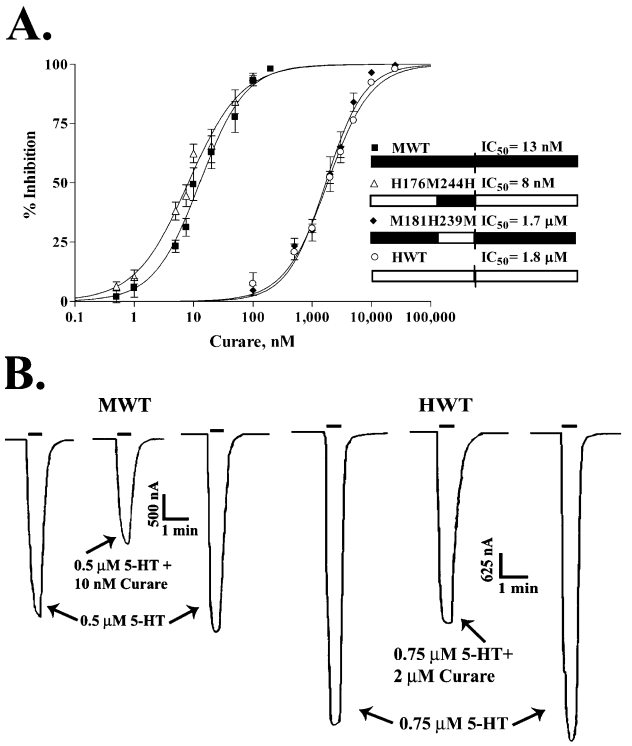

FIGURE 2: The actions of curare were examined in oocytes expressing mouse or human wild-type 5-HT_{3A} receptors or chimeric receptors. Human chimeric receptors in which the distal one-third of the N-terminus was replaced with the mouse receptor (H176M244H) or chimeric mouse receptors in which the distal one-third of the N-terminus was replaced with the human receptor (M181H239M) were also tested. The vertical line in the schematics depicting the receptor constructs demarcates the end of the N-terminus and the beginning of the first transmembrane domain. In panel A, stable baseline responses were obtained with an EC_{10} of 5-HT (0.5 μM, mouse WT and H176M244H; 0.75 μM, human WT and M181H239M), $n = 5-6$. Curare was coapplied with 5-HT for 30 s, and responses were expressed as a percent inhibition of the average baseline current. In panel B, representative tracings of 5-HT-evoked currents in the absence and presence of curare in mouse WT and human WT receptors are presented.

suggesting that both loops play a role in determining curare potency. Furthermore, the observation that all three chimeras had curare potency that was intermediate between those of mouse WT and human WT suggests that the presence of mouse orthologs in either loop can in part preserve higher curare potency.

The mirror image chimeras, in which mouse receptor orthologs were substituted on the human receptor background, were evaluated next (Figure 3C,D). In all three chimeras, the curare concentration response curves were shifted to the left relative to human WT. The curare IC_{50}'s for H-loop C+1 (40.07 ± 2.52 nM), H-loop F (131.8 ± 5.95 nM), and H-loop F+3 (82.45 ± 3.63 nM) were significantly lower than that of human WT (Table 1). H-loop F and H-loop F+3 IC_{50}'s were significantly different from each other (Table 1). Taken together, these results strongly support the idea that residues in both loops C and F underlie the differential curare potency in mouse and human receptors.

To determine whether the contributions of loops C and F to curare potency are energetically coupled, that is, nonadditive, we performed mutant thermodynamic cycle analysis (reviewed in ref *42*), Figure 3E. The mouse (panel a) and human (panel b) receptor analyses show the wild-type receptor in the left upper quadrant. The ΔG values upon mutation of loop C (right upper quadrant) or loop F (left lower quadrant) in the wild-type receptor are noted above the arrow between the wild-type receptor and chimera. Mutagenesis of the remaining loop in either chimera results in the chimera containing both mutant loops, lower right quadrant; the ΔG values are noted above the arrows between the chimeras. Finally, the arrow drawn diagonally between the wild-type receptor and the chimera with both substituted loops denotes the ΔG resulting from simultaneous loop substitutions. The reactions are numbered clockwise, beginning with the wild-type receptor. If the two mutations are independent, then the ΔG generated with simultaneous substitution of both loops should be equivalent to the addition of the two ΔG values generated from mutation of each loop, $\Delta G_{R1} + \Delta G_{R4} = \Delta G_{R5}$. Using the ΔG's for each step in the cycle, we can calculate a coupling energy (*42*) to determine whether loops C and F make independent contributions to curare binding:

$$\Delta G_{coupling} = \Delta G_{R1} - \Delta G_{R3} = \Delta G_{R2} - \Delta G_{R4}$$

In the case of the mouse background (Figure 3Ea), $\Delta G_{coupling} = -0.4 \pm 0.1$ kcal/mol, while in the case of the human background (Figure 3Eb), $\Delta G_{coupling} = -0.9 \pm 0.1$ kcal/mol. The coupling energies for the mouse and human receptors are small, suggesting that if the loops make interactions during the interaction of the receptor with curare, they are quite modest. However, it must be emphasized that these ΔG values were calculated from IC_{50} values, which may not be pure representations of antagonist affinity (*43*).

Given that the fold changes (13.3−45) in curare IC_{50}'s between human WT and the human chimeric receptors were greater than those between mouse WT and mouse chimeric receptors, human receptors containing individual mouse receptor orthologs were assessed for their roles in conferring curare potency. Nine differences in amino acid sequence are present in loop F+3, as indicated in Figure 1. Curare concentration response curves were generated in all nine human receptors containing point mutant mouse receptor orthologs, Figure 4A. Three mutant receptors had curare IC_{50}'s significantly lower than that of human WT (Table 1), but none of them had an IC_{50} equal to that of H-loop F. Within loop F, H-V202I (255.7 ± 7.27 nM) had a greater effect than H-K195E (546.0 ± 26.41 nM). The mutant H-L215F (1297 ± 40.05 nM) is located between loop F and loop C and had a more modest effect on curare potency. The double mutant receptor H-K195E,V202I (133.8 ± 6.38 nM) had an IC_{50} that was not significantly different from that of H-loop F (Figure 4B,C, Table 1). These results suggest that Lys195 and Val202 fully account for the loop F contribution to lower curare potency of the human 5-HT_{3A} receptor.

In order to evaluate H-K195E,V202I and its counterpart M-E200K,I207V more fully, we created three additional chimeras, H-loop C+1,K195E,V202I, H-loop C+1,V202I, and M-loop C+1,E200K,I207V. Addition of K195E and V202I together or V202I individually to the H-loop C+1 chimera was sufficient to achieve a curare IC_{50} equivalent to that of mouse WT. These results underscore the notion that the mouse receptor residues equivalent to Lys195 and Val202 in the human 5-HT_{3A} receptor (Glu200 and Ile207,

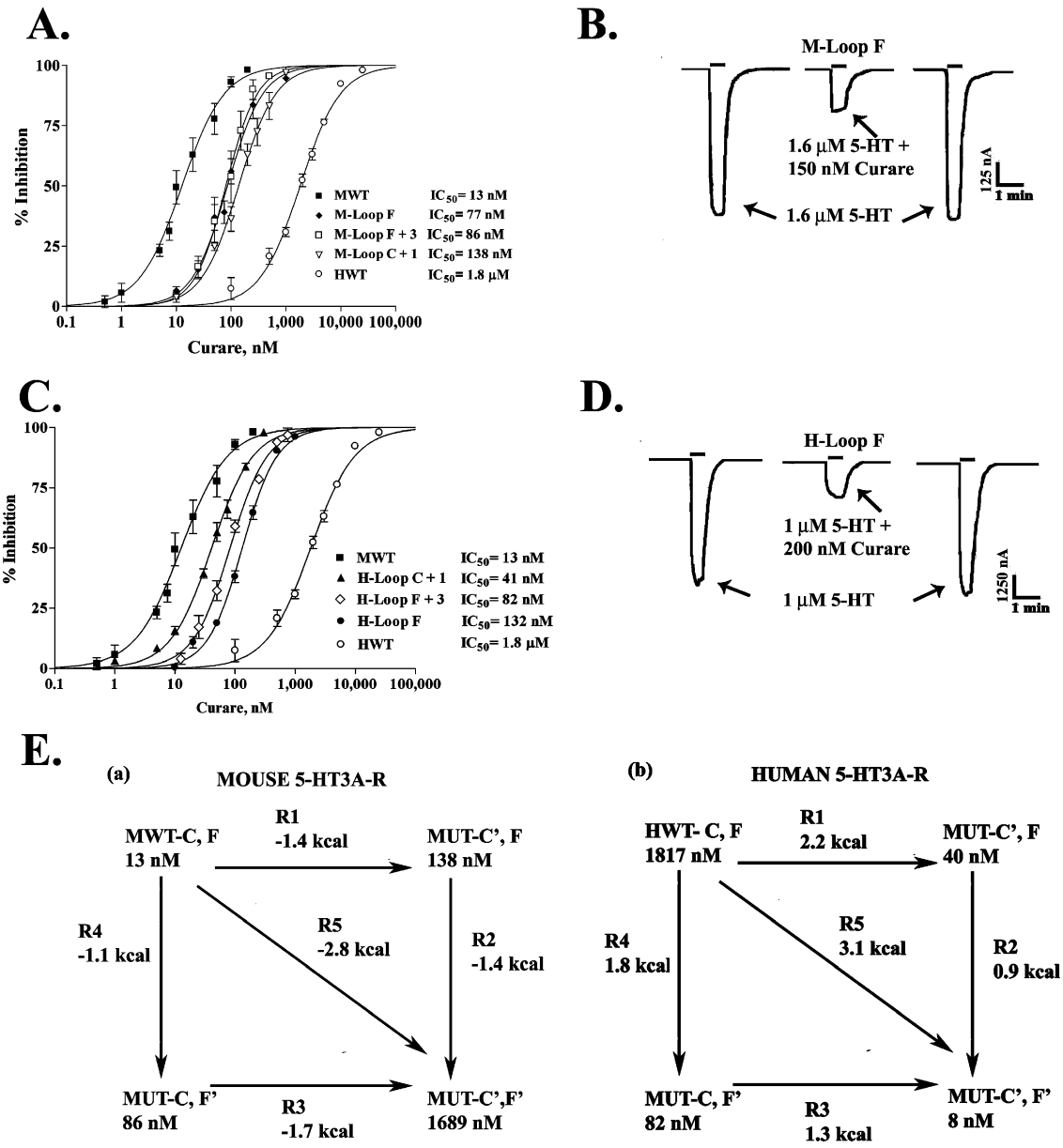

FIGURE 3: Curare concentration response curves were performed in oocytes expressing mouse−human or human−mouse 5-HT$_{3A}$ receptor chimeras and compared with that obtained in the wild-type receptors (as shown in Figure 2). These chimeras are described in the Figure 1 legend and in the Results. Curare was coapplied with 5-HT for 30 s, and responses were expressed as a percent inhibition of the average baseline current. In panel A, mouse chimeras containing human receptor orthologs were tested, $n = 6-7$. An EC_{10} 5-HT concentration was used (1.6 μM, M-loop F; 1.28 μM, M-loop F+3; 1.5 μM, M-loop C+1). One-way ANOVAs revealed that mouse WT and mouse chimeric receptor curare IC_{50}'s and human WT and mouse chimeric receptor curare IC_{50}'s were significantly different, $p < 0.001$. One-way ANOVA of Hill coefficients from the curare concentration response curves did not show significant difference, $p = 0.301$. In panel B, representative traces of 5-HT-evoked currents in the absence and presence of curare in M-loop F receptors are presented. In panel C, human chimeras containing mouse receptor orthologs were examined, $n = 5-6$. An EC_{10} 5-HT concentration was used (1 μM, H-loop C+1, H-loop F; 1.5 μM, H-loop F+3). One-way ANOVAs revealed that mouse WT and human chimeric receptor curare IC_{50}'s and human WT and human chimeric receptor curare IC_{50}'s were significantly different, $p < 0.001$. In panel D, representative traces of 5-HT-evoked currents in the absence and presence of curare in H-loop F receptors are shown. Panel E shows double mutant thermodynamic cycle analysis of mouse and human 5-HT$_{3A}$ receptors in which loop C+1, loop F+3, or both are mutated (C and F are wild-type and C′ and F′ are mutant).

respectively), both play an important role in determining curare potency. The chimera M-loop C+1,E200K,I207V had a curare IC_{50} of 1070 ± 50.8 nM, which is significantly less than that of human WT (Figure 5, Table 1). Given that H-L215F, a residue outside of loops C and F, had a significantly lower curare potency than human WT, substitution of the human ortholog at this position would likely further reduce the curare potency of M-loop C+1,E200K,-I207V. However, there is an 82-fold change between mouse WT and M-loop C+1,E200K,I207V IC_{50}'s and a 1.7 fold change between human WT and M-loop C+1,E200K,I207V IC_{50}'s. Thus, it is apparent that in the mouse receptor, of the non-loop C residues, Glu200 and Ile207 confer most of the curare potency.

A striking difference between our results and that of Hope et al., 1999, is the fold difference in curare potency in mouse and human 5-HT$_{3A}$ receptors. Hope and co-workers (1999) reported an approximately 1800-fold difference in IC_{50} values, whereas we report an approximately 140-fold difference. There were two notable differences in methodology

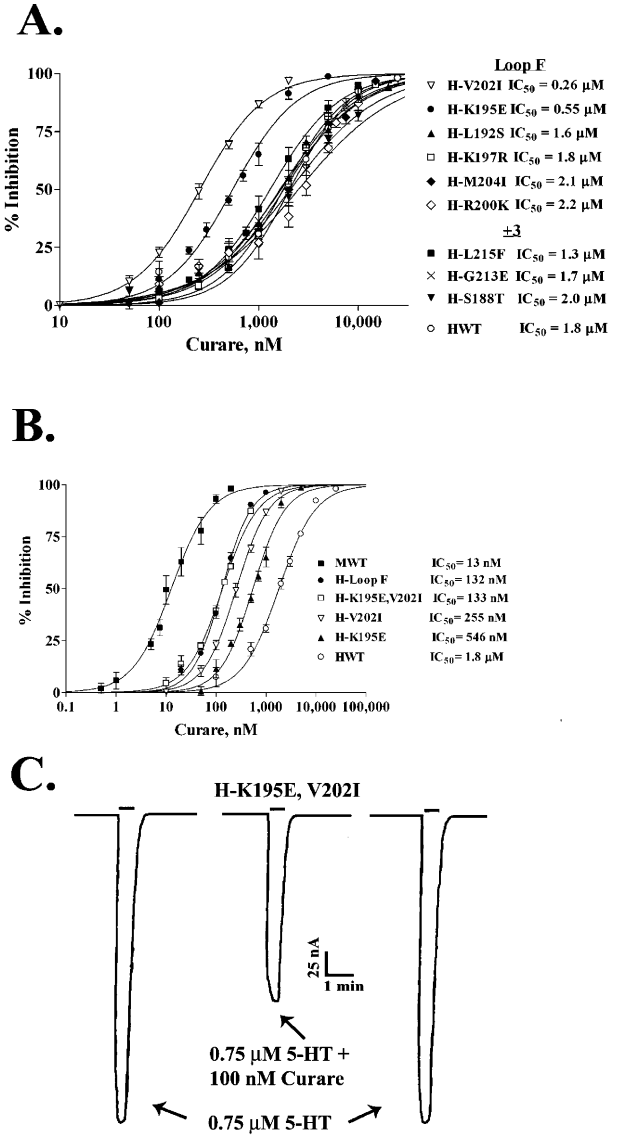

FIGURE 4: The role of loop F residues in conferring curare potency in mouse and human 5-HT_{3A} receptors was assessed. In panel A, curare concentration response curves were generated in oocytes expressing human point mutant receptors containing mouse receptor loop F orthologs. Three residues near but outside loop F (+3) that differ between mouse and human receptors were also assessed on the human receptor background, $n = 4-6$. An EC_{10} of 5-HT was used (0.7 μM, H-S188T; 0.75 μM, H-L192S; 0.25 μM, H-K195E; 1.75 μM, H-K197R and H-V202I; 1.5 μM, H-R200K; 1.25 μM, H-M204I; 0.55 μM, H-L215F; and 0.65 μM, H-G213E). One-way ANOVA of curare IC_{50}'s was significant, $p < 0.0001$. In panel B, a curare concentration response curve was generated in a mini-chimeric human receptor containing two mouse orthologs (H-K195E,V202I), $n = 5-9$; the 5-HT gating concentration (EC_{10}) was 0.75 μM. The concentration response curve was compared with that of the two point mutant receptors (shown in panel A) and the human chimeric receptors (shown in Figure 3C). One-way ANOVA of curare IC_{50}'s was significant, $p < 0.0001$. One-way ANOVA of Hill coefficients from the curare concentration response curves was significant, $p < 0.001$, but neither chimeric nor point mutant receptor values were significantly different from that of human WT, Student−Newman−Keul's post-hoc analysis, $p > 0.05$. In panel C, representative traces of H-K195E,V202I are shown.

between their study and the present one: (1) they preincubated oocytes with curare prior to application of 5-HT plus curare and (2) they used an EC_{50} concentration of 5-HT. To address whether either of these two differences played a role

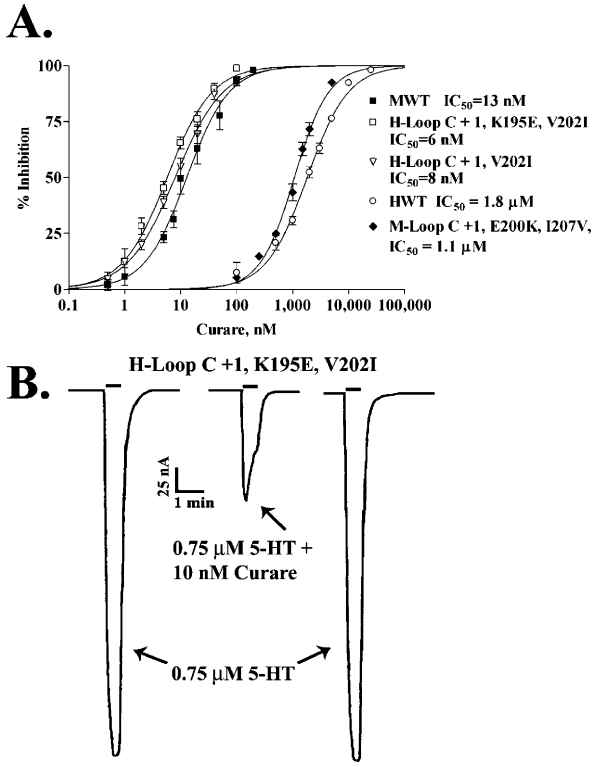

FIGURE 5: The combination of loop C+1 and two loop F receptor orthologs confer much of the curare potency of mouse and human 5-HT_{3A} receptors. In panel A, curare concentration response curves were generated in three chimeric receptors ($n = 4-10$) and compared with that obtained in mouse WT and human WT (shown in Figure 2A). Gating concentrations of 5-HT, an EC_{10}, were as follows: 1 μM, H-loop C+1,K195E,V202I; 0.75 μM, H-loop C+1,-V202I; 1.75 μM, M-loop C+1,E200K,I207V. There are five more residues in the N-terminus of the mouse 5-HT_{3A} receptor than in that of the human 5-HT_{3A} receptor; human Lys195 and Val202 are the orthologs of mouse Glu200 and Ile207, respectively. One-way ANOVA of mouse WT, H-loop C+1,K195E,V202I, and H-loop C+1,V202I IC_{50}'s was not significant, $p = 0.67$. In panel B, representative traces of 5-HT-mediated currents in the absence and presence of curare in H-loop C+1,K195E,V202I are displayed.

in lower fold differences in curare potency in our studies, we conducted two sets of experiments. In the first experiment, we preincubated mouse WT and human WT receptors with curare for 2 min prior to the application of 5-HT plus curare; the gating concentration of 5-HT was an EC_{10}. Curare IC_{50}'s were shifted leftward in both constructs, mouse WT (2.32 ± 0.13 nM) and human WT (1421 ± 70 nM), with an approximately 618-fold difference between the two. In the second experiment, we performed curare concentration response curves with an EC_{50} of 5-HT and no curare preincubation on mouse WT ($IC_{50} = 16.14 \pm 1.18$ nM) and human WT ($IC_{50} = 3279 \pm 50$ nM) receptors, obtaining a fold difference of approximately 203. These results suggest that pre-equilibration with curare plays a greater role than 5-HT gating concentration in determination of interspecies differences in curare potencies in our experiments.

DISCUSSION

In this study, we identified the role of loop F and confirmed the role of loop C (*39*) in determining the curare potency differences in mouse and human 5-HT_{3A} receptors. Both loops C and F play a major role, such that substitution of either loop C or F in the human receptor with mouse

receptor orthologs significantly enhances curare potency. Likewise, substitution of loop C or F of the mouse receptor with human receptor orthologs reduces curare IC_{50}'s to values intermediate between those of mouse WT and human WT, suggesting that mouse residues in either loop partially preserve the higher affinity of curare for the mouse receptor. Changes in free energy calculated with double mutant thermodynamic cycle analysis point to independent contributions of loops C and F in the mouse receptor in regulating curare potency. In the human receptor, there appears to be a modest interaction, with the mutation of one loop being greater than the mutation of an additional loop. In the human receptor, three residues mutated to the corresponding mouse orthologs enhanced curare potency. Two of these residues, H-Lys195 and H-Val202, are in loop F, whereas H-L215 is located between loops F and C. The human receptor containing the double mutant H-K195E,V202I had the same curare IC_{50} as that of the H-loop F chimera, suggesting that these two amino acids are sufficient to confer curare potency of mouse loop F receptor residues. Thus, our results demonstrate the importance of two loop F residues in determining curare potency in both mouse and human 5-HT_{3A} receptors. Across species of 5-HT_{3A} receptor, corresponding residues are either lysine or glutamic acid at the equivalent H-Lys195 residues and valine or isoleucine at the equivalent H-Val202 residues (*1*, *34*−*38*). The identity of these residues corresponds with curare potency, except in the case of the ferret receptor, which has human receptor equivalents at these positions and high curare potency (*37*). In contrast, in the 5-HT_{3B} subunit from human, mouse, and rat, aspartic acid is present at the human 5-HT_{3A} Lys195 equivalent, and alanine or serine is present at the human 5-HT_{3A} Val202 equiv (*2*, *3*, *52*). Likewise, in the human C, D, and E subunits, glutamic acid or threonine is present at the human 5-HT_{3A} Lys195 equivalent and valine, glycine, or isoleucine is present at the human 5-HT_{3A} Val202 equivalent (*4*, *5*).

Our finding that amino acids in the principal and complementary subunits of the 5-HT_{3A} receptor confer curare sensitivity parallels work done previously in the muscle-type and neuronal α7 nACh receptors. Both the α and γ/δ subunits are labeled by curare (*9*, *53*), and both subunits at the interface of the ligand binding domain are responsible for conferring curare affinity (*11*, *54*, *55*). Inasmuch as the defined 5-HT_3 receptor stoichiometry is a homomer of five A subunits (*1*) or a heteromer of two A and three B subunits (*56*), there are no parallels between these subunit interfaces and the nonequivalent α/δ and α/γ subunit interfaces in the nACh receptor that display differential curare or DMC affinities (*13*, *54*). However, invariant residues in loops D and E of the 5-HT_{3A} receptor, which correspond to residues in the nACh receptor identified as determinants of curare affinity (reviewed in ref *8*) have been examined. Mutations at these sites reduce curare binding affinity (*21*, *25*). The residues in loop F (loop G by Sine's nomenclature), δ-Lys161 and γ-Ser161, which are partly responsible for the subunit difference in DMC affinity (*13*), correspond to Trp190 in the human 5-HT_{3A} receptor, which is invariant across species. No residues that confer curare sensitivity in the nACh receptors correspond to human 5-HT_{3A} receptor Lys195 and Val202. However, H-Val202 corresponds to Gly189 in the chicken and Gly167 in the human α7 nACh receptor loop F, which have been characterized in two reports. Mutations at this residue influence partial agonist potency and efficacy (*57*, *58*).

Our results are consistent with other reported findings on curare sensitivity of the 5-HT_{3A} receptor. First, Hope et al. (*39*) found in mouse and human chimeric 5-HT_{3A} receptors that loop C substitutions were not sufficient to confer mouse or human wild-type receptor curare sensitivity. Their observation that substitution of individual loop C residues of the mouse receptor with human receptor orthologs only produced modest changes in curare potency (10-fold or less) is likely attributable to an interaction among residues within loop C. In addition, based upon the results presented in our study, we suggest another explanation for their results. As demonstrated in human and mouse chimeric receptors in this study, mouse residues in loops C and F make a substantial contribution to high curare potency. Therefore, their presence in either loop of mutant mouse receptors should in part preserve curare potency. We suggest that this is the reason why mouse receptors containing either loop C or F human equivalents in our study or mouse receptors containing loop C human equivalents in their study have such high curare potency. Our results differ from that of Hope et al. (*39*) in that they reported approximately 1800-fold difference in curare IC_{50}'s between mouse WT and human WT, whereas we observed approximately 140-fold difference in curare potency. In experiments designed to account for the differences, we found that preincubation of oocytes with curare enhanced its potency to a greater degree in mouse WT than in human WT, with a fold change of approximately 618. In contrast, with a higher gating concentration of 5-HT (EC_{50}), the fold difference in curare potency between mouse and human receptors was approximately 203, similar to that observed with an EC_{10} of 5-HT. While pre-equilibration is clearly more important than 5-HT concentration in determining interspecies curare potency differences in the present study, other unidentified factors must be at play, given that our fold differences in any case are substantially lower than that previously reported. However, it is important to note that despite these differences, we adhered to internally consistent sets of measurements in our experiments to arrive at interpretations of our results. Finally, the approach used in the present study necessarily only identifies residues that determine curare potency that differ between mouse and human receptors; curare-sensitive residues that are identical in human and mouse receptors presumably play equivalent roles in curare binding in receptors from these two species. Since loops A, B, and D are identical in mouse and human 5-HT_{3A} receptors, our approach would not identify resides in any of these loops that are important in curare binding and therefore is not in contradiction with our previous findings regarding the importance of loop A and D residues (*21*, *27*, *28*). The three residues in loop E that differ between mouse and human 5-HT_{3A} receptors likely play no role in conferring curare potency. The chimera M181H239M, which contains the three loop E mouse receptor orthologs, has the same curare potency as human WT. This observation is supported by the work of Venkataraman et al. (*25*) who examined curare displacement of [^{3}H]-granisetron binding in mouse 5-HT_{3A} receptors containing alanine mutations in loop E. Only substitution at Y140 (invariant across species) affected the curare K_i.

Changes in the 5-HT EC_{50}'s in the chimeric and point mutant receptors relative to wild-type receptors were small (Table 1) but statistically significant and support the possible role of loops C and F in the conformational changes associated with ion channel opening. Significant changes in agonist EC_{50}'s and partial agonist efficacies with mutation are routinely used to assess a residue's possible role in gating. A previous study examined alanine substitutions at Phe226, Ile228, and Tyr234 in loop C and demonstrated that the relative efficacies of the partial agonist 2-methyl 5-HT and 5-HT are altered, suggesting a role of these residues in gating (*18*). Likewise, mutations of Tyr234 to unnatural amino acids point to the aromatic ring as playing a role in both binding and gating (*17*). Recent work in our laboratory (*59*) has shown that the presence of mouse or human orthologs in the distal one-third of the N-terminus of the 5-HT_{3A} receptor determines whether 3-(2-hydroxy,4-methoxybenzylidene)-anabaseine is a partial agonist or antagonist, respectively. Thus, residues in loop C or F or both likely participate in the gating process. Consistent with a role of loop C in the gating process, in the case of the *Aplysia* AChBP (*45*), loop C sticks out away from the bulk of the protein in the unliganded form but moves closer to the body of the protein in the agonist-bound form, clamping down over the agonist. Whether the residues identified as curare-sensitive in the present study also participate in gating is currently under study. The residue H-Val202, and its ortholog, M-Ile207, identified as a residue important for curare affinity in the present study, correspond to Gly189 in the chicken and human α7 nACh receptor loop F. This residue influences potency and efficacy of 3-(2,4-dimethoxybenzylidene)-anabaseine (*58*). Likewise, Gly189 also regulates partial agonist efficacy of imidacloprid (*57*). Finally, substituted cysteine accessibility studies of the $GABA_A$ receptor suggest that Val180 of the α1 subunit, which corresponds to 5-HT_{3A} receptor H-Val202 and M-Ile207, is one of three residues in loop F that act as a dynamic element during agonist-mediated ion channel opening (*60*). Collectively, these results lend support to the idea that both loops C and F of the 5-HT_{3A} receptor are integral parts of the ligand-binding domain, with contact points for antagonists and agonists, which are associated with initial molecular motions that culminate in ion channel flux.

The three-dimensional structure of the acetylcholine binding protein (AChBP) (*31*) has been used in the generation of homology models of the N-terminal domains of the 5-HT_{3A} receptor (*27*, *31*, *32*). These models have significantly improved our understanding of the generalized architecture of the agonist binding domain and the roles of amino acids in loops A−F as putative contact points for agonists and antagonists. Maksay and co-workers (*31*) have compared mouse and human 5-HT_{3A} receptor models and suggest that loop C orthologs, mouse Asp229/human Glu224 and mouse Ile230/human Ser225, by virtue of differences in side chain length and size, respectively, not only change intramolecular interactions but also alter the spatial orientation of curare. They propose that curare moves deeper into the ligand binding domain of the human receptor because of less steric hindrance provided by serine than isoleucine at human residue 225. This disrupts a crucial H-bond of curare with H-Glu224. Interestingly, their model predicts that loop F of the mouse receptor has no interaction with curare but that

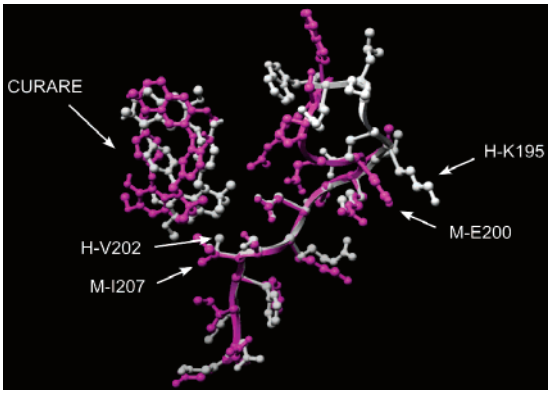

FIGURE 6: Molecular model of the mouse 5-HT_{3A} receptor ligand-binding domain. Shown are loop F from the mouse (magenta) and human (gray) 5-HT_{3A} receptors with curare docked in the ligand-binding domain. The two residues shown to be important determinants of species differences in curare sensitivity (M-Glu200/H-Lys195 and M-Ile207/H-Val202) are indicated.

Asp199 of the human receptor interacts with the tertiary nitrogen. However, this model was constructed using a structure of the AChBP that is now known to be in the agonist-bound conformation, in which loop C is clamped down over the agonist. In the apo and antagonist-bound forms of the AChBP, loop C has rotated away from the bulk of the receptor like a paddle (*44*, *61*), allowing greater access to the ligand-binding site. In our own modeling and docking studies, we were unable to get curare to fit into the binding site as a high-affinity complex using models derived using the agonist-bound form of the AChBP as the template but were able to do so using models derived from the apo and antagonist-bound forms of the AChBP as the template (*28*). In light of this, the relevance of the model of Maksay et al. (*31*) to this study is unclear.

We have created homology models of the mouse and human receptors using the structures of the apo and methyllycaconitine-bound forms of the *Aplysia* AChBP (*45*) as templates and carried out docking simulations of curare with both receptors. While the modeled structures of both receptors are very similar (as expected from the high degree of homology between the mouse and human receptors), the structure of loop F is quite different in the two receptors, with the human loop F sticking further away from the core of the receptor in the region containing residues M-Arg196/H-Arg191 to M-Arg202/H-Lys197. Comparison of the potential hydrogen bonds in the two structures shows that this region of the mouse receptor makes many more H-bonds with other residues in the receptor than the human segment, presumably causing the mouse loop to be more compact. We examined the positions of M-Glu200/H-Lys195 and M-Ile207/H-Val202 the 5-HT_{3A} receptor in our models of the curare-5-HT_{3A} receptor complex, which was selected from the lowest-energy dockings from AutoDock based on the results of extensive double-mutant cycle analysis (*28*). Figure 6 shows the curare−receptor complex with M-Glu200/H-Lys195 and M-Ile207/H-Val202 shown in gray (human receptor) and magenta (mouse receptor). In these models M-Ile207/H-Val202 is close to the aromatic ring in curare containing the 6′ methoxy group, and the longer isoleucine side chain may contribute to the higher affinity of the mouse receptor. However, in these models M-Glu200/H-Lys195 protrude away from curare, and based on these models, it is

more likely that the residues at this position influence either the local environment or local structure rather than making direct physical contact with curare. However, given that loop F was poorly resolved in the AChBP structure, suggesting that loop F is somewhat flexible (*30*), and given the uncertainties associated with the exact positions of side chains in structural models derived from homology modeling (*62*), any interpretation based on the structural models is speculative and requires further experimental studies employing double-mutant cycle analysis (*28*, *63*) with curare analogs before any firm conclusions can be made. Nonetheless, the difference in the models for loop F in the two receptors is consistent with the notion that loop F is an important determinant of curare affinity.

In summary, our findings underscore the importance of loop F in determining curare potency in the 5-HT_{3A} receptor. In addition, they demonstrate the importance of conservative, as well as the expected nonconservative substitutions, in conferring drug potency. The unexpected finding that H-V202I would produce the largest shift in curare potency of any of the point mutants tested reveals the power of the interspecies mutational analysis performed. Future experiments employing mutant receptors, curare analogs, or both coupled with additional molecular modeling studies of bound curare in the mouse and human 5-HT_{3A} receptors will shed light on the role of critical residues in loops C and F in shaping the three-dimensional architecture of the ligand recognition site.

REFERENCES

1. Maricq, A. V., Peterson, A. S., Brake, A. J., Myers, R. M., and Julius, D. (1991) Primary structure and functional expression of the 5-HT_3 receptor, a serotonin-gated ion channel, *Science 254*, 432−437.
2. Davies, P. A., Pistis, M., Hanna, M. C., Peters, J. A., Lambert, J. J., Hales, T. G., and Kirkness, E. F. (1999) The 5-HT_{3B} subunit is a major determinant of serotonin receptor function, *Nature 397*, 359−363.
3. Dubin, A. E., Huvar, R., D'Andreas, M. R., Pyati, J., Zhu, J. Y., Koy, K. C., Wilson, S. J., Galindo, J. E., Glass, C.A., Lin, L., Jackson, M. R., Lovenberg, T. W., and Erlander, M. G. (1999) The pharmacological and functional characteristics of the serotonin 5-HT(3A) receptor are specifically modified by a 5-HT(3B) receptor subunit, *J. Biol. Chem. 274*, 30799−30810.
4. Karnovsky, A. M., Gotow, L. F., McKinley, D. D., Piechan, J. L., Ruble, C. L., Mills, C. J., Schellin, K. A. B., Slightom, J. L., Fitzgerald, L. R., Benjamin, C. W., and Roberds, S. L. (2003) A cluster of novel serotonin receptor 3-like genes on human chromosome 3, *Gene 319*, 137−148.
5. Niesler, B., Frank, B., Kapeller, J., and Rappold, G. A. (2003) Cloning, physical mapping and expression analysis of the human 5-HT3 serotonin receptor-like genes HTR3C, HTR3D and HTR3E, *Gene 319*, 101−111.
6. Morales, M., and Wang, S. D. (2002) Differential composition of 5-hydroxytryptamine3 receptors synthesized in the rat CNS and peripheral nervous system, *J. Neurosci. 22*, 6732−6741.
7. Reeves, D. C., and Lummis, S. C. R. (2002) The molecular basis of the structure and function of the 5-HT_3 receptor: a model ligand-gated ion channel (review), *Mol. Membr. Biol. 19*, 11−26.
8. Sine, S. M. (2002) The nicotinic receptor ligand binding domain, *J. Neurobiol. 53*, 431−446.
9. Pedersen, S. E., and Cohen, J. B. (1990) *d*-Tubocurarine binding sites are located at α-γ and α-δ subunit interfaces of the nicotinic acetylcholine receptor, *Proc. Natl. Acad. Sci. U. S. A. 87*, 2785−2789.
10. Filatov, G. N., Aylwin, M. L., and White, M. M. (1993) Selective enhancement of the interaction of curare with the nicotinic acetylcholine receptor, *Mol. Pharmacol. 44*, 237−241.
11. Sine, S. M., Quiram, P., Papanikolaou, F., Kreienkamp, H.-J., and Taylor, P. (1994) Conserved tyrosines in the α subunit of the nicotinic acetylcholine receptor stabilize quaternary ammonium groups of agonists and curariform antagonists, *J. Biol. Chem. 269*, 8808−8816.
12. Chiara, D. C., and Cohen, J. B. (1997) Identification of amino acids contributing to high and low affinity d-tubocurarine sites in the *Torpedo* nicotinic acetylcholine receptor, *J. Biol. Chem. 272*, 32940−32950.
13. Sine, S. M. (1993) Molecular dissection of subunit interfaces in the acetylcholine receptor: Identification of residues that determine curare sensitivity, *Proc. Natl. Acad. Sci. U. S. A. 90*, 9436−9440.
14. Papineni, R. V. L., and Pedersen, S. E. (1997) Interaction of *d*-tubocurarine analogs with mouse nicotinic acetylcholine receptor, *J. Biol. Chem. 272*, 24891−24898.
15. Willcockson, I. U., Hong, A., Whisenant, R. P., Edwards, J. B., Wang, H., Sarkar, H. K., and Pedersen, S. E. (2002) Orientation of *d*-tubocurarine in the muscle nicotinic acetylcholine receptor-binding site, *J. Biol. Chem. 277*, 42249−42258.
16. Schreiter, C., Hovius, R., Costioli, M., Pick, H., Kellenberger, S., Schild, L., and Vogel, H. (2003) Characterization of the ligand binding site of the 5-HT_3 receptor, *J. Biol. Chem. 278*, 22709−22715.
17. Beene, D. L., Price, K. L., Lester, H. A., Dougherty, D. A., and Lummis, S. C. R. (2004) Tyrosine residues that control binding and gating in the 5-Hydroxytryptamine$_3$ receptor revealed by unnatural amino acid mutagenesis, *J. Neurosci. 24*, 9097−9104.
18. Suryanarayanan, A., Joshi, P. R., Bikadi, Z., Muthalagi, M., Kulkarni, T. R., Gaines, C., and Schulte, M. K. (2005) The loop C region of the murine 5-HT_{3A} receptor contributes to the differential actions of 5-Hydroxytryptamine and *m*-Chlorophenylbiguanide, *Biochemistry 44*, 9140−9149.
19. Thompson, A. J., Price, K. L., Reeves, D.C., Chan, S. L., Chau, P.-L., and Lummis, S. C. R. (2005) Locating an antagonist in the 5-HT_3 receptor binding site using modeling and radioligand binding, *J. Biol. Chem. 280*, 20476−20482.
20. Boess, F. G., Steward, L. J., Steele, J. A., Liu, D., Reid, J., Glencorse, T. A., and Martin, I. L. (1997) Analysis of the ligand binding site of the 5-HT_3 receptor using site directed mutagenesis: importance of glutamate 106, *Neuropharmacology 36*, 637−647.
21. Yan. D., Schulte, M. K., Bloom, K. E., and White, M. M. (1999) Structural features of the ligand-binding domain of the serotonin 5-HT_3 receptor, *J. Biol. Chem. 274*, 5537−5541.
22. Spier, A. D., and Lummis, S. C. R. (2000) The role of tryptophan residues in the 5-Hydroxytryptamine$_3$ receptor ligand binding domain, *J. Biol. Chem. 275*, 5620−5625.
23. Steward, L. J., Boess, F. G., Steele, J. A., Liu, D., Wong, N., and Martin, I. L. (2000) Importance of phenylalanine 107 in agonist recognition by the 5-hydroxytryptamine(3A) receptor, *Mol. Pharmacol. 57*, 1249−1255.
24. Beene, D. L., Brandt, G. S., Zhong, W., Zacharias, N. M., Lester, H. A., and Dougherty, D. A. (2002) Cation−π interactions in ligand recognition by serotonergic (5-HT_{3A}) and nicotinic acetylcholine receptors: The anomalous binding properties of nicotine, *Biochemistry 41*, 10262−10269.
25. Venkataraman, P., Venkatachalan, S. P., Joshi, P. R., Muthalagi, M., and Schulte, M. K. (2002) Identification of critical residues in loop E in the 5-HT_{3AS}R binding site, *BMC Biochem. 3*, 15.
26. Price, K. L., and Lummis, S. C. R. (2004) The role of tyrosine residues in the extracellular domain of the 5-Hydroxytryptamine$_3$ receptor, *J. Biol. Chem. 279*, 23294−23301.
27. Yan, D., and White, M. M. (2005) Spatial orientation of the antagonist granisetron in the ligand binding site of the 5-HT_3 receptor, *Mol. Pharmacol. 68*, 365−371.
28. Yan, D., Meyer, J. K., and White, M. M. (2006) Mapping residues in the ligand-binding domain of the 5-HT_3 receptor onto d-tubocurarine structure, *Mol. Pharmacol. 70*, 571−578.
29. Thompson, A. J., Padgett, C. L., and Lummis, S. C. R. (2006) Mutagenesis and molecular modeling reveal the importance of the 5-HT_3 receptor F-loop, *J. Biol. Chem. 281*, 16576−16582.
30. Brejc, K., van Dijk, W. J., Klaassen, R. V., Schuurmans, M., van Der Oost, J., Smit, A. B., and Sixma, T. K. (2001) Crystal structure of an ACh-binding protein reveals the ligand-binding domain of nicotinic receptors, *Nature 411*, 269−276.
31. Maksay, G., Bikadi, Z., and Simonyi, M. (2003) Binding interactions of antagonists with 5-Hydroxytryptamine$_{3A}$ receptor models, *J. Recept. Signal Transduction 23*, 255−270.

32. Reeves, D. C., Sayed, M. F. R., Chau, P.-L., Price, K. L., and Lummis, S. C. R. (2003) Prediction of 5-HT3 receptor agonist-binding residues using homology modeling, *Biophys. J. 84*, 2338−2344.
33. Peters, J. A., Hales, T. G., and Lambert, J. J. (2005) Molecular determinants of single-channel conductance and ion selectivity in the Cys-loop family: insights from the 5-HT3 receptor, *Trends Pharmacol. Sci. 26*, 587−594.
34. Isenberg, K. E., Ukhum, I. A., Holstad, S. G., Jafri, S., Uchida, U., Zorumski, C. F., and Yang, J. (1993) Partial cDNA cloning and NGF regulation of a rat 5-HT_3 receptor subunit, *NeuroReport 5*, 121−124.
35. Miyake, A., Mochizuki, S., Takemoto, Y., and Akuzawa, S. (1995) Molecular cloning of human 5-Hydroxytryptamine$_3$ receptor: heterogeneity in distribution and function among species, *Mol. Pharmacol. 48*, 407−416.
36. Lankiewicz, S., Lobbitz, S., Lobitz, N., Wetzel, C. H. R., Rupprecht, R., Gisselmann, G., and Hatt, H. (1998) Molecular cloning, functional expression, and pharmacological characterization of 5-hydroxytryptamine$_3$ receptor cDNA and its splice variants from guinea pig, *Mol. Pharmacol. 53*, 202−212.
37. Mochizuki, S., Watanabe, T., Miyake, A., Saito, M., and Furuichi, K. (2000) Cloning, expression, and characterization of ferret 5-HT-(3) receptor subunit, *Eur. J. Pharmacol. 399*, 97−106.
38. Jensen, T. N., Nielsen, J., Frederiksen, K, and Ebert, B. (2006) Molecular cloning and pharmacological characterization of serotonin 5-HT_{3A} receptor subtype in dog, *Eur. J. Pharmacol. 538*, 23−31.
39. Hope, A. G., Belelli, D., Mair, I. D., Lambert, J. J., and Peters, J. A. (1999) Molecular determinants of (+)-tubocurarine binding at recombinant 5-hydroxytryptamine$_{3A}$ receptor subunits, *Mol. Pharmacol. 55*, 1037−1043.
40. Mochizuki, S., Miyake, A., and Furuichi, K. (1999) Identification of a domain affecting agonist potency of meta-chlorophenylbiguanide in 5-HT_3 receptors, *Eur. J. Pharmacol. 369*, 125−132.
41. Machu, T. K., Hamilton, M. E., Frye, T. F., Shanklin, C. L., Harris, M. C., Sun, H., Tenner, Jr., T. E., Soti, F. S., and Kem, W. R. Benzylidene analogs of anabaseine display partial agonist and antagonist properties at the mouse 5-hydroxytryptamine(3A) receptor, *J. Pharmacol. Exp. Ther. 299*, 1112−1117.
42. Ackers, G. K., and Smith, F. R. (1985) Effects of site-specific amino acid modification on protein interactions and biological function, *Annu. Rev. Biochem. 54*, 597−629.
43. Colquhoun, D. (1998) Binding, gating, affinity and efficacy: the interpretation of structure-activity relationships for agonists and of the effects of mutating receptors, *Br. J. Pharmacol. 125*, 924−947.
44. Sali, A., and Blundell, T. (1993) Comparitive protein modeling by satisfaction of spatial restraints, *J. Mol. Biol. 234*, 779−815.
45. Hansen, S., Sulzenbacher, G., Huxford, T., Marchot, P., Taylor, P., and Bourne, Y. (2005) Structures of *Aplysia* AChBP complexes with nicotinic agonists and antagonists reveal distinctive binding interfaces and conformations, *EMBO J. 24*, 3635−3646.
46. Cantescu, A. A., Shelenkov, A. A., and Dunbrack, R. L. (2003) A graph-theory algorithm for rapid protein side-chain prediction, *Protein Sci. 12*, 2001−2014.
47. Sippl, M. J. (1993) Recognition of errors in three-dimensional structures of proteins, *Proteins 17*, 355−362.
48. Morris, G., Goodsell, D., Huey, R., Hart, W., Belew, R., and Olson, A. (1998) Automated docking using Lamarckian genetic algorithm and an empirical free energy binding free energy function, *J. Comput. Chem. 19*, 1639−1662.
49. Gasteiger, J., and Marsili, M. (1980) Iterative partial equalization of orbital electronegativity- A rapid access to atomic charges, *Tetrahedron 36*, 3219−3228.
50. Ferrara, P., Gohlke, H., Price, D. J., Klebe, G., and Brooks, C. L., III (2004) Assessing scoring functions for protein−ligand interactions, *J. Med. Chem. 47*, 3032−3047.
51. Pettersen, E., Goddard, T., Huang, C., Couch, G., Greenblatt, D., Meng, E., and Ferrin, T. (2004) UCSF Chimera: A visualization system for exploratory research and analysis, *J. Comput. Chem. 25*, 1605−1612.
52. Hanna, M. C., Davies, P. A., Hales, T. G., and Kirkness, E. F. (2000) Evidence for expression of heteromeric 5-HT_3 receptors in rodents, *J. Neurochem. 75*, 240−247.
53. Pedersen, S. E., Dreyer, E. B., and Cohen, J. B. (1986) Location of the ligand-binding sites on the nicotinic acetylcholine receptor α-subunit, *J. Biol. Chem. 261*, 13735−13743.
54. Blount, P., and Merlie, J. P. (1989) Molecular basis of the two nonequivalent ligand binding sites of the muscle nicotinic acetylcholine receptor, *Neuron 3*, 349−357.
55. O'Leary, M. E., Filatov, G. N., and White, M. M. (1994) Characterization of d-tubocurarine binding site of *Torpedo* nicotinic acetylcholine receptor, *Am. J. Physiol. 266*, C648−C653.
56. Barrera, N. P., Herbert, P., Henderson, R. M., Martin, I. L., and Edwardson, J. M. (2005) Atomic force spectroscopy reveals the stoichiometry and subunit arrangement of 5-HT3 receptors, *Proc. Natl. Acad. Sci. U. S. A. 102*, 12595−12600.
57. Shimomura, M., Yokota, M., Okumura, M., Matsuda, K., Akamatsu, M., Sattelle, D. V., and Komai, K. (2003) Combinatorial mutations in loops D and F strongly influence responses of the nicotinic acetylcholine receptor to imidacloprid, *Brain Res. 991*, 71−77.
58. Stokes, C., Papke, J. K. P., Horenstein, N. A., Kem, W. R., McCormack, T. J., and Papke, R. L. (2004) The structural basis for GTS-21 selectivity between human and rat nicotinic α7 receptors, *Mol. Pharmacol. 66*, 14−24.
59. Zhang, R., White, N. A., Soti, F. S., Kem, W. R., and Machu, T. K. (2006) N-terminal domains in mouse and human 5-Hydroxytryptamine$_{3A}$ receptors confer partial agonist and antagonist properties to benzylidene analogs of anabaseine, *J. Pharmacol. Exp. Ther. 37*, 1276−1284.
60. Newell, J. G., and Czajkowski, C. (2003) The GABAA receptor α1 subunit pro^{174} − Asp^{191} segment is involved in GABA binding and channel gating, *J. Biol. Chem. 278*, 13166−13172.
61. Celie, P. H., Kasheverov, I. E., Mordvintsev, D. Y., Hogg, R. C., van Nierop, P., van Elk, R., van Rossum-Fikkert, S. E., Zhmak, M. N., Bertrand, D., Tsetlin, V., Sixma, T. K., and Smit, A. B. (2005) Crystal structure of nicotinic acetylcholine receptor homolog AChBP in complex with an alpha-conotoxin PnIA variant, *Nat. Struct. Mol. Biol. 12*, 582−588.
62. Al-Lazikani B., Jung J., Xiang Z., and Honig B. (2001) Protein structure prediction, *Curr. Opin. Chem. Biol. 5*, 51−56.
63. Hidalgo, P., and MacKinnon, R. (1995) Revealing the architecture of a K^+ channel pore through mutant cycles with a peptide inhibitor, *Science 268*, 307−310.

BI0616100